# Elastic Scattering of Protons by Single Isotopes

CLYDE B. FULMER
*Oak Ridge National Laboratory,* Oak Ridge, Tennessee*
(Received August 17, 1961)

Differential cross sections for the elastic scattering of 22.2-Mev protons were measured for 20 targets of predominantly single isotopic composition at $\sim 2\frac{1}{2}$-deg intervals over the angular range of 20°–150°. The targets ranged from $Mg^{24}$ to $U^{238}$ and included three pairs of isobars. Cross sections for elastic scattering of 16.4- and 9.5-Mev protons were also measured for $Ni^{64}$ and $Zn^{64}$ at $\sim 2\frac{1}{2}$-deg intervals over the angular range of 25°–120°. The 9.5-Mev data for $Ni^{64}$ and $Zn^{64}$ show differences in the positions of maxima and minima of the elastic scattering angular distributions that are consistent with a dependence of real nuclear potential well depth on the nuclear symmetry parameter $(N-Z)/A$. The 22.2-Mev data indicate that the positions of minima and maxima of the elastic scattering angular distributions are not appreciably influenced by closed nucleon shells nor by variation of $(N-Z)/A$. The 22.4-Mev data indicate that elastic scattering at large angles is influenced by nuclear deformation.

## INTRODUCTION

THE elastic scattering of protons by atomic nuclei has been extensively studied.[1–29] The interest generated by the systematic study of Cohen and Neidigh[7] of proton-nucleus elastic scattering and the stimulus provided by the successes of the nuclear optical model[30–36] have resulted in the accumulation of data at a large number of proton energies and a wide range of nuclear mass. The data reported here were obtained with two main purposes in mind.

A possible dependence of the real nuclear potential well depth, $V$, on the nuclear symmetry parameter $(N-Z)/A$, i.e.,

$$V=\{V_1\pm[(N-Z)/A]V_2\}, \tag{1}$$

for protons and neutrons, respectively, has been suggested by Green and Sood[37] and by Lane.[38] Sliv and Volchock[39] have investigated average nuclear potential parameters by studying nuclear level data for nuclei with double-closed shells plus or minus one nucleon. On the basis of this study these authors have concluded that the potential parameters are the same for all nuclei that lie on the stability curve; for nuclei off the stability curve they suggest that there is a change in the depth of the proton potential that is given by

$$\Delta V=(a/A)(N-N_{st}), \tag{2}$$

where $N$ is the neutron number, $N_{st}$ is the neutron number for the isobar on the stability curve, $A$ is the mass number, and the quantity $a\sim 80$ Mev. Optical-model analyses of proton-nucleus elastic scattering data[31,32,40] have shown that maxima and minima in the angular distributions occur at angular positions which are determined mainly by $VR^n$, where $R$ is the nuclear radius and $n$ is a parameter that varies with

* Operated for the U. S. Atomic Energy Commission by Union Carbide Corporation.

[1] J. W. Burking and B. T. Wright, Phys. Rev. **82**, 451 (1951).
[2] B. T. Wright, University of California Radiation Laboratory Report UCRL-2422, 1953 (unpublished).
[3] C. J. Baker, J. N. Dodds, and D. H. Simmons, Phys. Rev. **85**, 1051 (1952).
[4] P. C. Gugelot, Phys. Rev. **87**, 525 (1952).
[5] L. M. Goldman, Phys. Rev. **89**, 349 (1953).
[6] W. E. Burcham, W. M. Gibson, A. Hossain, and J. Rotblat, Phys. Rev. **92**, 1266 (1953).
[7] B. L. Cohen and R. V. Neidigh, Phys. Rev. **93**, 282 (1954).
[8] G. Fischer, Phys. Rev. **96**, 704 (1954).
[9] R. G. Freemantle, D. J. Prowse, A. Hossain, and J. Rotblat, Phys. Rev. **96**, 1270 (1954).
[10] R. G. Freemantle, D. J. Prowse, and J. Rotblat, Phys. Rev. **96**, 1268 (1954).
[11] J. Leahy, University of California Radiation Laboratory Report UCRL-3273, 1956 (unpublished).
[12] I. E. Dayton and G. Schrank, Phys. Rev. **101**, 1358 (1956).
[13] D. A. Bromley and N. S. Wall, Phys. Rev. **114**, 525 (1959).
[14] G. Gerstein, J. Niederer, and K. Strauch, Phys. Rev. **108**, 427 (1957).
[15] C. B. Fulmer, Phys. Rev. **116**, 418 (1959).
[16] M. K. Brussel and J. H. Williams, Phys. Rev. **114**, 525 (1959).
[17] R. A. Vanetsian, A. D. Klyucharev, and E. D. Fedchenko, Atomnaya Energ. **6**, 663 (1959).
[18] C. A. Preskitt and W. P. Alford, Phys. Rev. **115**, 1700 (1959).
[19] R. W. Boom and J. R. Richardson, Phys. Rev. **115**, 1700 (1959).
[20] K. Kikuchi, S. Kobayashi, and K. Matsuda, J. Phys. Soc. Japan **14**, 121 (1959).
[21] C. Hu *et al.*, Tokyo University Institute for Nuclear Study Report INSJ-20, 1959 (unpublished).
[22] N. M. Hintz, Phys. Rev. **106**, 1201 (1957).
[23] N. N. Pacherov, Ukrain. Fiz. Zhur. **4**, 313 (1959); **4**, 318 (1959).
[24] A. K. Valter *et al.*, J. Exptl. Theoret. Phys. (U.S.S.R.) **38**, 1419 (1960).
[25] Y. Oda, M. Takeda, C. Hu, and S. Kato, J. Phys. Soc. Japan **14**, 1255 (1959).
[26] R. Beurtey *et al.*, Nuclear Phys. **13**, 397 (1959).
[27] A. P. Klyucharev and N. Ya. Rutkevich, J. Exptl. Theoret. Phys. **38**, 285 (1960).
[28] S. Kobayashi, K. Matsuda, Y. Nagahara, Y. Oda, and N. Yamamuro, J. Phys. Soc. Japan **15**, 1151 (1960).
[29] J. Benveniste, R. Booth, and A. Mitchell, Phys. Rev. **123**, 1818 (1961).
[30] R. W. Woods and D. S. Saxon, Phys. Rev. **95**, 577 (1954).
[31] R. M. Sternheimer, Phys. Rev. **100**, 886 (1955).
[32] A. E. Glassgold *et al.*, Phys. Rev. **106**, 1207 (1957).
[33] A. E. Glassgold and P. J. Kellog, Phys. Rev. **107**, 1372 (1957).
[34] A. E. Glassgold and P. J. Kellog, Phys. Rev. **109**, 1291 (1958).
[35] M. A. Melkanoff, S. A. Moszkowski, J. S. Modvik, and D. S. Saxon, Phys. Rev. **101**, 507 (1956).
[36] J. S. Nodvik and D. S. Saxon, Phys. Rev. **117**, 1539 (1960).
[37] A. E. S. Green and P. C. Sood, Phys. Rev. **111**, 1147 (1958).
[38] A. M. Lane, *Proceedings of the International Conference on Nuclear Physics, Paris, July, 1958* (Dunod, Paris, 1959), pp. 32–34.
[39] L. A. Sliv and B. A. Volchock, J. Exptl. Theoret. Phys. (U.S.S.R.) **36**, 539 (1959).
[40] J. S. Nodvik, *Proceedings of the International Conference on the Nuclear Optical Model, Florida State University Studies, No. 32* (The Florida State University, Tallahassee, Florida, 1959).

proton energy. It would seem that the experimental study of proton-nucleus elastic scattering from isobars should be the most direct way to obtain experimental information about the magnitude of $V_2$ in Eq. (1) or the quantity $a$ in (2). Part of the data reported here were obtained with this motivation.

A large part of the previously reported elastic scattering data was obtained with targets of natural isotopic abundances. This leaves some uncertainty as to whether some details of proton-nucleus elastic scattering are obscured by the averaging effect of multiple-isotope targets. In a few cases[15–17,19,26] data were obtained from single isotope targets. Except for the work reported in reference 17, each of these studies has been limited to a narrow range of nuclear mass. For the data reported here, targets of predominantly single isotopic composition and wide range of nuclear mass and atomic number were used in an attempt to study, experimentally, the effects of nuclear mass, closed nucleon shells, and nuclear deformation on proton-nucleus elastic scattering.

## EXPERIMENTAL

The 22.2-Mev external proton beam of the ORNL 86-in. cyclotron was used. For some of the experiments, incident protons of lower energy were obtained by using aluminum absorbers in the beam path.

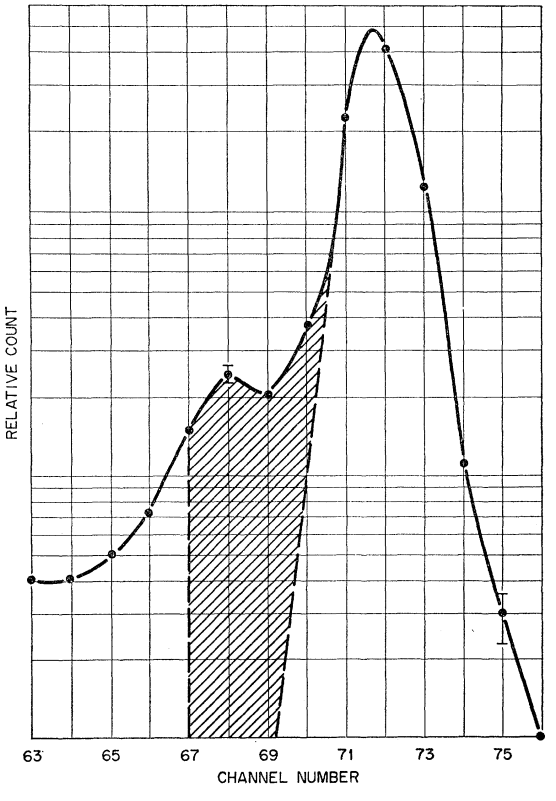


FIG. 1. Part of the pulse-height spectrum obtained from a $Co^{59}$ target with detection angle of 30°. The area under the curve and to right of shaded area was used to determine the elastic scattering cross section. The shaded area extends from $-Q=1.5$ Mev to the elastic peak (see text).

A 24-in. diam scattering chamber was used. The chamber consists of two cylindrical parts with an O-ring and ball-bearing race between the two cylinders. The upper cylinder may be rotated about the scattering chamber axis, with a chain and motor, without disturbing the vacuum.

The proton beam enters the scattering chamber through a horizontal pipe near the top of the lower cylinder, is collimated, passes through a thin foil of target material at the axis of the scattering chamber, and is collected in a Faraday cup which monitors the beam. For these experiments a $\frac{1}{4}$-in. diam collimator was used to define the incident beam. The target foils are positioned by a remotely-controlled target wheel; thus targets may be changed without interrupting cyclotron operation. Outgoing particles are observed at one of several ports located in the upper cylinder. The axis of each port intersects the incident proton beam at the target position.

For some of the data, the proton beam passed through aluminum absorbers before being collimated at the entrance of the scattering chamber. This provided a beam of incident protons of lower energy. When the proton energy was thus reduced from 22.2 Mev to 9.5 Mev the available beam intensity was reduced by a factor of 20. When the incident proton energy was reduced to 16.4 Mev, the available beam intensity was reduced by a factor of 5.

For these experiments a NaI(Tl) scintillation detector was used. Pulse-height analysis was used to identify elastically scattered protons, and the count for each data point was obtained by numerical integration of the peak that corresponds to the elastically scattered protons in the pulse-height spectrum. The width of this peak for protons elastically scattered from a thin gold foil at a forward angle was 3% (full width at half maximum) or less (usually $2\frac{1}{2}$%) during these experiments. The peak width results from a combination of detector energy resolution and energy spread of the incident proton beam. Inelastically scattered protons that leave the target nuclei with $\lesssim$500-kev excitation are not resolved from elastically scattered protons. The numerical integration of the elastic peaks might include some contributions (for targets with levels below ~500 kev) from inelastic scattering. An effort to minimize this effect was made by symmetrizing the peak as is illustrated in Figs. 1 and 2. Some idea of the errors that might result from inelastic scattering that excites levels that are of too low energy to be resolved from the elastic peak can be had by examining Figs. 1 and 2. The known levels of $Co^{59}$ are all above 1 Mev, and hence inelastically scattered protons are resolved from the elastic peak. The hash-marked areas in Figs. 1 and 2 correspond to negative $Q$ values between ~1 and ~1.5 Mev which include the known levels at 1.097, 1.189, 1.289, and 1.432 Mev. If the integrals

under these portions of the curves were included in the elastic peaks, the integrals of the latter would be increased ~5% at 30° (Fig. 1) and ~40% at 148° (Fig. 2). These values are probably larger than any inelastic contributions to the elastic scattering data reported here. The inelastic scattering contributions are believed to be less than 5% at forward angles.

Some of the elastically scattered protons that enter the detector induce nuclear reactions in the detector; the scintillation pulses from these events are not included in the elastic peak. The magnitude of this effect for 22-Mev protons in a NaI crystal was investigated[41]; the effect is ~0.8% of the elastic scattering cross section.

Data for each target were obtained by proceeding through the angular range of the data with changes of ~5° in the angular position of the detector between successive counts. A second progression through the angular range was subsequently made with detector settings ~5° apart and near the midpoints of successive detector settings for the initial sweep through the angular range. Thus the repeatability of the data was checked, and angular distributions were determined by data obtained at ~2½-degree intervals.

The target foils were oriented 45° with respect to the incident proton beam. For angles $\leq 120°$, transmission data were obtained (i.e., all protons that entered the detector passed through both surface planes of the target foils). For angles $>120°$, reflection data were obtained (i.e., all protons that entered the detector passed through the same surface plane in entering and leaving the target foils). The angular aperture of the collimator for the detector is approximately 1°, and the relative angular positions of the detector can be read to within ¼°.[42] Counting statistics are 8% or better for all data points, and better than 5% for almost all points.

The data obtained from numerical integration of the elastic peaks were corrected for center-of-mass motion, etc., before angular distributions and cross sections were determined.

The Mg target foil is natural magnesium which is 78.8% $Mg^{24}$. The $Ni^{58}$ target foil is natural nickel which is 68.0% $Ni^{58}$. The $Fe^{58}$ target foil is enriched to 78% $Fe^{58}$. The other target foils used in this work are higher than 90% abundant in the principal isotope.

One of the targets that was studied is $Ho^{165}$ in the form of a thin holmium oxide foil.[43] Protons elastically scattered by oxygen and by holmium were sufficiently resolved at angles $\gtrsim 35°$ for the elastic scattering due to Ho to be determined from the pulse-height spectra. A spectrographic analysis indicated no impurities (other than oxygen) of abundances large enough to contribute significantly to the measured proton elastic scattering cross sections.

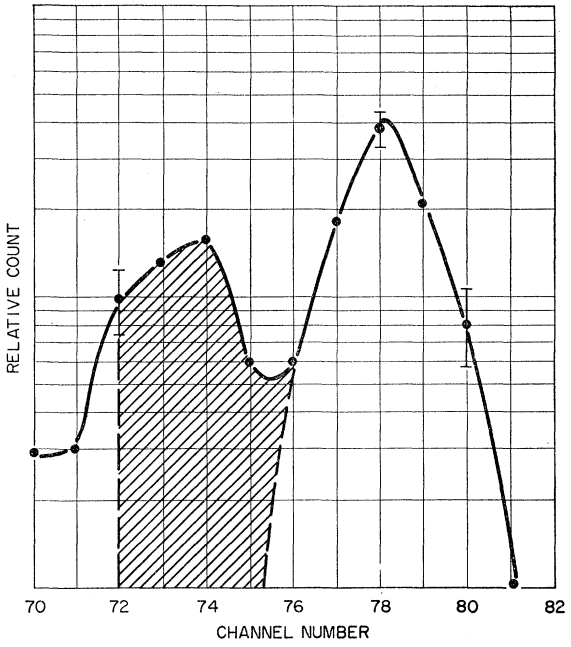


FIG. 2. Part of the pulse-height spectrum obtained from a $Co^{59}$ target with detection angle of 148°. The area under the curve and to right of shaded area was used to determine the elastic scattering cross section. The shaded area extends from $-Q=1.5$ Mev to the elastic peak (see text).

The $Ni^{64}$, $Zn^{64}$, $Cd^{116}$, $Sn^{116}$, and $Pb^{208}$ target foils were prepared by the Isotopes Division of Oak Ridge National Laboratory. The $Fe^{57}$ target foil was prepared at Argonne National Laboratory. The $Fe^{58}$ target foil was prepared at Los Alamos Scientific Laboratory. Both the $Fe^{57}$ and $Fe^{58}$ foils were used in another experiment.[44] The other target foils used in this work were obtained from commercial sources.

## RESULTS AND DISCUSSION

### Elastic Scattering of Protons by Isobars

Elastic scattering angular distributions are shown for 22.2-, 16.4-, and 9.5-Mev protons on $Ni^{64}$ and $Zn^{64}$ in Fig. 3, for 22.2-Mev protons on $Fe^{58}$ and $Ni^{58}$ in Fig. 4, and for 22.2-Mev protons on $Cd^{116}$ and $Sn^{116}$ in Fig. 5. These data were obtained for the purpose of determining whether the proposed effect of the nuclear symmetry parameter on the real nuclear potential well depth is observable in experiments of this kind. It is reasonable to assume that the same radius parameter applies to two isobars. Thus differences in the positions of maxima and minima in the elastic scattering angular distributions could be interpreted as the result of a difference in potential encountered by incoming protons.

[41] J. B. Ball and C. B. Fulmer (to be published).

[42] Absolute measurements of detection angles may be in error by as much as 1 degree due to uncertainty of the positions of the beam axis.

[43] The author gratefully acknowledges that the holmium foil was supplied by D. A. Bromley.

[44] C. D. Goodman, J. B. Ball, and C. B. Fulmer (to be published).

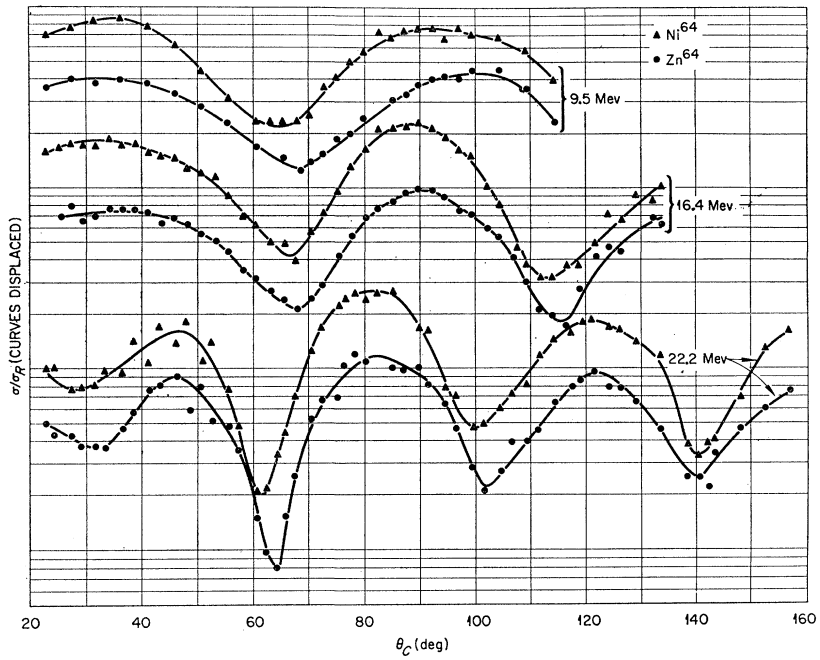


FIG. 3. Elastic scattering angular distribution for 9.5-, 16.4-, and 22.2-Mev protons on $Ni^{64}$ and $Zn^{64}$. The curves are ratios of elastic scattering cross sections to Rutherford scattering cross sections.

In the 22.2-Mev data of Fig. 3,[45] the maxima and minima for $Zn^{64}$ occur at the same or slightly larger angles than for $Ni^{64}$. The fact that on the average the features of the angular distributions occur at slightly larger angles for $Zn^{64}$ suggests that the real potential depth for $Ni^{64}$ is greater than for $Zn^{64}$. Such small differences as exist, however, might be attributed to the difference in Coulomb potential, $V_C$, for the two nuclei. The optical-model potential consists of a real nuclear potential, an imaginary nuclear potential, and a Coulomb potential. Since the Coulomb potential is positive while the real nuclear potential is negative, a larger value of $V_C$ should produce an effect similar to that of a smaller value of $V$. $V_C$ for $Zn^{64}$ is $\sim$0.5 Mev larger than for $Ni^{64}$ at the nuclear surface (if the nuclear radius is assumed to be $1.5\times10^{-13}$ cm$\times A^{\frac{1}{3}}$). The nuclear symmetry parameter, $(N-Z)/A$, is smaller for $Zn^{64}$ than for $Ni^{64}$, and therefore, according to Eq. (1), $V$ should be smaller for $Zn^{64}$ than for $Ni^{64}$. Hence, the small difference in the positions of maxima and minima of the elastic scattering angular distributions for 22.2-Mev protons on $Ni^{64}$ and $Zn^{64}$ does not provide good evidence for a nuclear symmetry parameter effect on $V$. An examination of 22.2-Mev proton elastic scattering data for $Fe^{58}$ and $Ni^{58}$ (Fig. 4) and for $Cd^{116}$ and $Sn^{116}$ (Fig. 5) shows no significant differences between the positions of maxima and minima for either pair of isobars. Thus from the 22.2-Mev data for these three pairs of isobars one cannot see convincing evidence of a dependence of $V$ on $(N-Z)/A$.

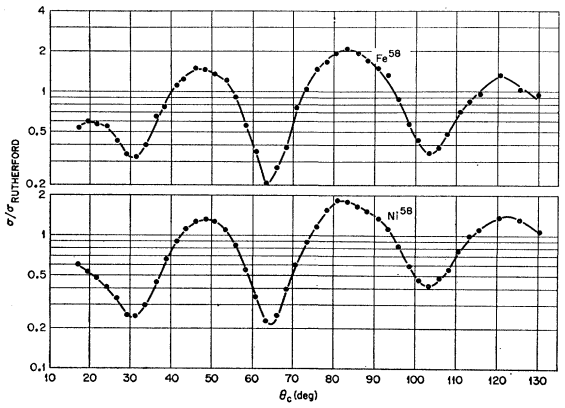


FIG. 4. Elastic scattering angular distributions for 22.2-Mev protons on $Fe^{58}$ and $Ni^{58}$. The curves are ratios of elastic scattering cross sections to Rutherford scattering cross sections.

The dependence of proton elastic scattering on the magnitude of $V$ was investigated theoretically by Glassgold *et al.*[32] for 9.72-Mev protons and subsequently was investigated by Glassgold and Kellog[33,34] at 17 Mev and at 40 Mev. Although quantitative results of the studies at 17 Mev and 40 Mev were not published, the investigations indicated that the effect of $V$ on proton elastic scattering decreases with proton energy.

The 9.5-Mev data of Fig. 3 were obtained for two reasons: (a) the dependence of the positions of maxima and minima in proton elastic scattering on $V$ is larger at lower proton energy, and hence a difference in the magnitude of $V$ for the two isobars would produce a larger effect to be observed experimentally; and (b) the experimental data could be compared with the results of the investigation of Glassgold *et al.*[32]

[45] A preliminary report of these data is included in the *Proceedings of the International Conference on the Nuclear Optical Model, Florida State University Studies, No. 32* (The Florida State University, Tallahassee, Florida, 1959).

The energy threshold for $Zn^{64}(p,n)$ reactions is 7.88 Mev and for $Ni^{64}(p,n)$ reactions it is 2.46 Mev. Since the proton energy at 9.5 Mev is ~1.6 Mev above the $(p,n)$ reaction threshold for $Zn^{64}$ and ~7 Mev above for $Ni^{64}$, it is reasonable to assume that compound-elastic scattering events will contribute more to the measured elastic scattering cross sections in the case of $Zn^{64}$ than in that of $Ni^{64}$. The contribution is probably negligible for $Ni^{64}$. From the proton reaction cross-section data[29] for $Cu^{63}$ and $Cu^{65}$ it is apparent that compound-elastic scattering does not represent a significant part of the total reaction cross section for protons slightly above the $(p,n)$ threshold. The cross section for compound-elastic scattering, however, may be significant when compared to the shape-elastic scattering cross section. Therefore the possible influence of compound-elastic scattering on $Zn^{64}$ data must be considered in the 9.5-Mev data of Fig. 3. If it is assumed that compound elastic scattering makes an isotropic contribution to the shape elastic scattering angular distribution, then it can be shown by elementary calculus techniques that the effect on a $\sigma/\sigma_R$ angular distribution is to shift minima to smaller angles and maxima to larger angles.

A comparison of the 9.5-Mev data for $Ni^{64}$ and $Zn^{64}$ with the published curves of Glassgold *et al.*[32] which show a typical variation of the positions of angular features of proton-nucleus elastic scattering with $V$ will yield an estimate of $V_2$ [see Eq. (1)]. The average effect of an increase of 1 Mev in $V$ was shown in reference 32 to displace a maximum or a minimum to a 2.1-deg smaller angle (for angles greater than ~50°). In Fig. 3 the minimum near 65° occurs at ~4-degree smaller angle for $Ni^{64}$ than for $Zn^{64}$ (for the 9.5-Mev data); the maximum near 100° occurs at ~6-degree smaller angle for $Ni^{64}$ than for $Zn^{64}$. The average difference of these two is 5°. This can be interpreted to imply that the real potential is ~2.4 Mev deeper for $Ni^{64}$ than for $Zn^{64}$. If the 0.5-Mev difference in $V_C$ is taken into account, ~1.9-Mev difference in $V$ may be attributed to a nuclear symmetry dependence of $V$;

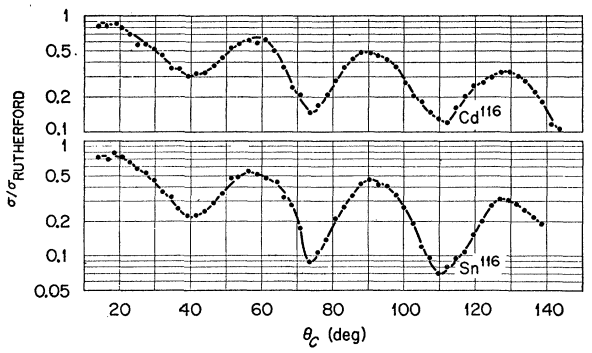


FIG. 5. Elastic scattering angular distributions for 22.2-Mev protons on $Cd^{116}$ and $Sn^{116}$. The curves are ratios of elastic scattering cross sections to Rutherford scattering cross sections.

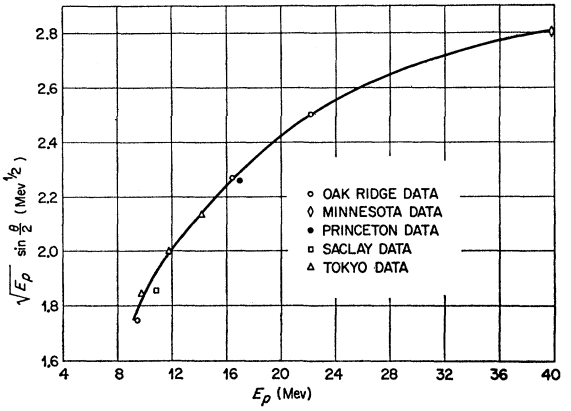


FIG. 6. Values of momentum transfer for protons at minima of elastic scattering angular distributions near 60° for 9.5–40 Mev protons on $A \sim 64$ nuclei. See reference 16 for Minnesota data, reference 12 for Princeton data, reference 26 for Saclay data, and reference 21 for Tokyo data.

this leads to an estimate that the magnitude of $V_2$ is ~30 Mev. This is in good agreement with the value suggested by Green[37] and in very poor agreement with the differences in the real potential depth that were suggested by Sliv and Volchock.[39] If Eq. (2) is applied to $Ni^{64}$ and $Zn^{64}$, a difference of real potential depth of 7.5 Mev is indicated.

Although the data are not extensive enough to determine the value of $V_2$ with great accuracy and optical model analyses of the data are not available at this time, the 9.5-Mev data of Fig. 3 appear to provide experimental evidence of the existence of a nuclear symmetry dependence of $V$, and they suggest $V_2$ of Eq. (1) be ~30 Mev. This is in qualitative agreement with the proton elastic scattering data obtained by Benveniste *et al.*[29] for protons at several energies in the range of 7–12 Mev on $Cu^{63}$ and $Cu^{65}$; shifts in the positions of minima and maxima were observed to be two or three times as large as can be attributed to the change in $A^{\frac{1}{3}}$ for the two isotopes.

There are also curves in Fig. 3 that show proton elastic scattering angular distributions for $Ni^{64}$ and $Zn^{64}$ at 16.5-Mev proton energy. These data show less evidence of a difference in $V$ for the two isobars than the 9.5-Mev data.

From the results of this survey it seems reasonable to conclude that evidence for differences in real nuclear potential well depth are not manifested in 22-Mev proton elastic scattering by isobars, but there is evidence of a difference in $V$ in the 9.5-Mev data. The lack of evidence for the effect at 22-Mev proton energy may be partially attributed to the decreasing influence of $V$ on elastic scattering with increasing proton energy. It may be that the nuclear symmetry effect on $V$ washes out at higher energy. The 9.5-Mev data suggest the desirability of additional proton elastic scattering data for isobars at ~10-Mev proton energy.

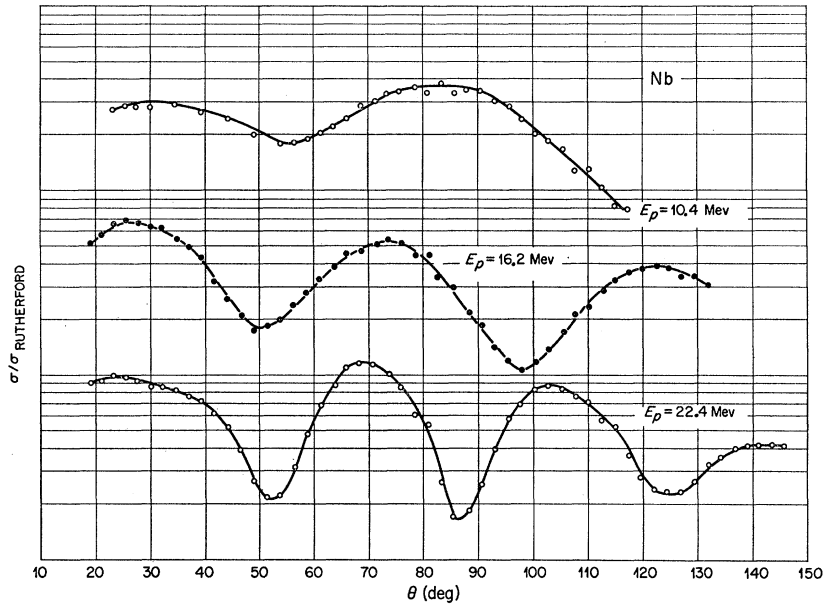


FIG. 7. Elastic scattering angular distributions for 10.4-, 16.4-, and 22.4-Mev protons on $Nb^{93}$. The curves are ratios of elastic scattering cross sections to Rutherford scattering cross sections. There is no significance to the vertical position of each curve.

## Elastic Scattering of Protons of Variable Energy

The simple Born approximation treatment[46] of nucleon-nucleus elastic scattering leads to an expression of the type

$$\sigma(\theta)\sim[CJ_1(KR)]^2, \tag{3}$$

where the Bessel function argument is the product of the interaction radius $R$ and the momentum transfer $K$. This expression is an approximation that is usually considered to be valid only for small angles. Although it does not take into account Coulomb effects or nuclear surface diffuseness, in numerous cases of elastic scattering of protons of a single energy value by nuclei of a range of mass values, relation (3) has been demonstrated to agree with experimental results in that the positions of maxima and minima vary approximately as $A^{-\frac{1}{3}}$. It is interesting to compare the effect of varying $K$ in relation (3) while $R$ remains constant.

The simple Born approximation treatment implies that if the interaction radius remains constant and the momentum of the incident nucleon is varied, a particular feature of the elastic scattering angular distribution should occur at angular positions so that the momentum transfer will remain constant. The minima for $A=64$ nuclei near 65° (Fig. 3) show a gross deviation from this; the proton momentum at $E=22.2$ Mev is ~50% greater than at 9.5 Mev, while the angular positions of the minima are different by only ~10%. In Fig. 6 is shown a plot of a compilation of experimentally determined positions of the minima near 65°, in angular distributions of protons of various energies on $A\sim64$ nuclei. The ordinate is proportional to the momentum transfer $K$. If the Born approximation treatment were closely followed, the graph would be one of constant ordinate. It appears in Fig. 6 that this behavior may prevail at higher proton energies, but it definitely does not for proton energies below 40 Mev.

The effect of variation of initial proton energy on proton-nucleus elastic scattering angular distributions was examined at another region of nuclear mass. In Fig. 7 are shown experimentally determined angular distributions for 10.4-, 16.2-, and 22.4-Mev protons elastically scattered by $Nb^{93}$. The minima between

TABLE I. Experimentally determined differential elastic scattering cross sections for 22.2-Mev protons on various targets.

| Target | Center-of-mass Scattering angle (deg) | $d\sigma/d\Omega$ (mb/sr) |
|---|---|---|
| $Mg^{24}$ | 89.7 | 5.91 |
| $Al^{27}$ | 89.7 | 6.31 |
| $V^{51}$ | 91.1 | 11.8 |
| $Mn^{55}$ | 91.0 | 10.1 |
| $Fe^{57}$ | 91.0 | 10.5 |
| $Fe^{58}$ | 91.0 | 9.42 |
| $Ni^{58}$ | 91.0 | 9.77 |
| $Co^{59}$ | 91.0 | 11.4 |
| $Ni^{64}$ | 90.9 | 10.2 |
| $Zn^{64}$ | 90.9 | 10.7 |
| $Nb^{93}$ | 90.6 | 4.52 |
| $Rh^{103}$ | 90.6 | 2.79 |
| $Cd^{116}$ | 90.5 | 10.2 |
| $Sn^{116}$ | 90.5 | 8.7 |
| $Ta^{181}$ | 90.4 | 7.58 |
| $Au^{197}$ | 90.3 | 7.66 |
| $Pb^{208}$ | 90.3 | 5.8 |
| $Bi^{209}$ | 90.3 | 10.4 |
| $U^{238}$ | 90.2 | 15.6 |

[46] See, for instance, B. T. Feld, H. Feshbach, M. L. Goldberger, H. Goldstein, and V. F. Weisskopf, Atomic Energy Commission Report NYO 636, 1951 (unpublished).

50° and 60° change position only slightly over the range of proton energy; the second minima change angular position more with proton energy; and the third maxima change angular position with proton energy (see the 16.2- and 22.4-Mev curves in Fig. 7) in a manner that is in fair agreement with simple diffraction theory. The better agreement between the observed angular distributions and the predictions of the simple Born approximation treatment is also obtained for $A=64$ nuclei (Fig. 3) at large angles.

## Elastic Scattering of 22.2-Mev Protons by Single Isotopes

Elastic scattering angular distributions of 22.2-Mev protons from targets of principally single isotopic composition are shown in Fig. 8. The data include targets ranging from Mg to U. The curves are arbitrarily displaced, and consequently only relative cross sections are shown. Absolute differential cross sections for a number of the targets for one detection angle near 90° are given in Table I.

The $Ni^{64}$ data in Fig. 8 were obtained by repeating the data run on that target after Fig. 3 was prepared. The scattering of the data points around 40°–50° in Fig. 3 is not repeated in Fig. 8. The measured angular distributions are the same, however. The $Zn^{64}$ data of Fig. 8 are the same as that of Fig. 3. The $U^{238}$ data of Fig. 7 are published[15] but are included here for comparison with the other angular distributions. The data of Fig. 8 cover a large range of nuclear mass; data from several closed shell nuclei are included, and the data include angular distributions from spherical and deformed nuclei.

Figure 9 shows a partial digest of Fig. 8. The angular positions of maxima and minima are plotted vs $A^{-\frac{1}{3}}$. Several closed shell nuclei are indicated in Fig. 9.

The data of Fig. 8 as summarized in Fig. 9 show that positions of maxima and minima in the angular distributions vary smoothly with mass of the scattering nuclei and are almost linearly dependent on (nuclear radius)$^{-1}$ for forward scattering. The data for closed shell nuclei do not show any differences that can be attributed to closed shells as was suggested by the work of Brussel and Williams.[16] For forward angles the positions of maxima and minima in the elastic scattering angular distributions are not sensitive to nuclear deformations. The data of Fig. 8 show that in general the amplitude of the oscillations in the angular distribution curves decreases with increasing nuclear mass.

## Effect of Nuclear Deformation on Proton-Nucleus Elastic Scattering

In the scattering process the momentum transfer increases with the angle through which the particles are scattered; thus the particles that are scattered through large angles in nucleon-nucleus elastic scattering probe the nuclear potential more deeply than those that are scattered through small angles. The data of Fig. 6 show angular distributions of 22.2-Mev protons elastically scattered by both spherical nuclei (e.g., $Sn^{116}$ and $Pb^{208}$) and deformed nuclei (e.g., $Mg^{24}$, $Al^{27}$, $Ho^{165}$, and $Ta^{181}$). These data show evidence of an effect due to a spheroidal nuclear potential on proton-nucleus elastic scattering. The data obtained with spherical nuclei exhibit well-defined maxima and minima throughout the angular range of the data; the amplitude of the oscillations in the angular distributions is almost as great at large angles as at small angles. The data from deformed nuclei also exhibit angular distributions that have well-defined features at forward angles, but the maxima and minima are not well defined

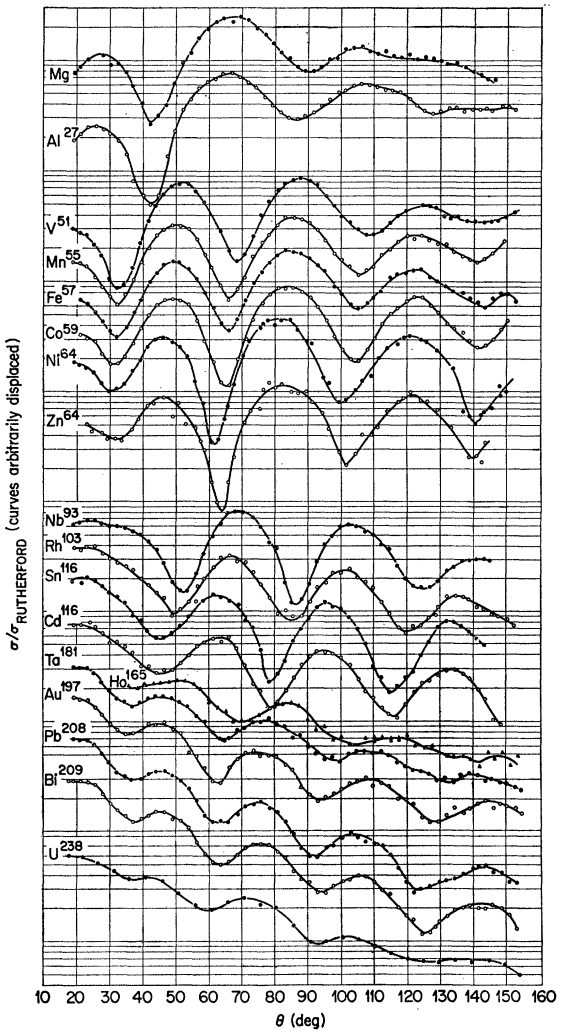


FIG. 8. Elastic scattering angular distributions for 22.2-Mev protons on various targets. The curves are ratios of elastic scattering cross sections to Rutherford scattering cross sections.

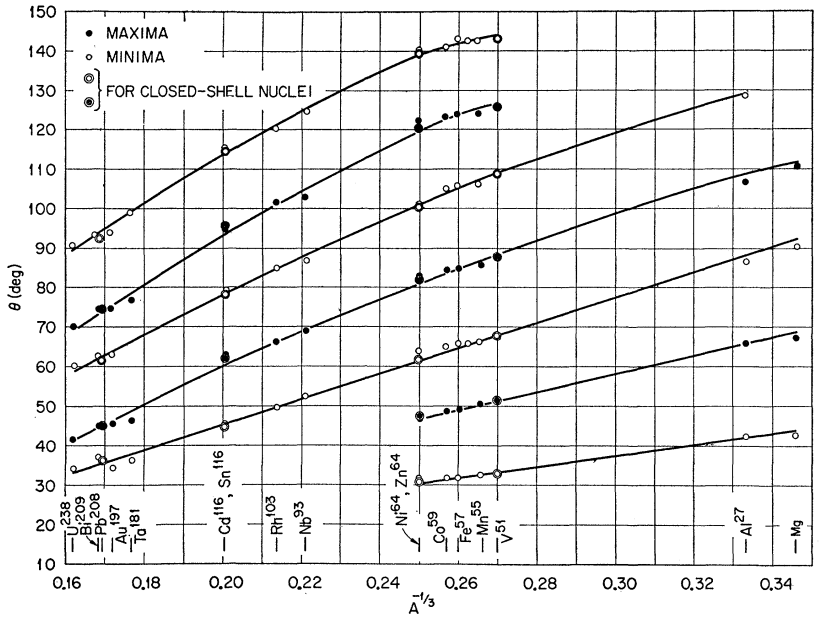


FIG. 9. Angular location of maxima and minima in elastic scattering angular distributions for 22.2-Mev protons as functions of $A^{-\frac{1}{3}}$ for the target nucleus.

at angles $\gtrsim 100°$. In the case of the deformed nuclei, the amplitudes of the oscillations in the angular distribution are significantly smaller at large angles.

If compound-nucleus elastic scattering were a large part of the measured elastic scattering cross section, this could conceivably result in the featureless character of the angular distributions at large angles. This certainly does not apply for the case of the heavy targets such as $Ta^{181}$; the $(p,n)$ threshold is 0.96 Mev, and the density of levels is large. Nor does it seem to apply in the case of the light targets; the $(p,n)$ thresholds for $Mg^{24}$ and $Al^{27}$ are 14.8 Mev and 6.1 Mev, respectively, and the angular distributions are very similar.